



## **Lipped channel cold-formed steel columns: “all-in-one” design approach including the buckling interaction models LG, LD, DG and LDG**

Eduardo de M. Batista<sup>1</sup>, Gustavo Y. Matsubara<sup>2</sup>, Marcílio Sousa de Rocha Freitas<sup>3</sup>, Victor A. M. de Faria<sup>4</sup>, André L. R. Brandão<sup>5</sup>

### **Abstract**

The present research investigates the structural behavior of lipped channel cold-formed steel (CFS) columns with a focus on the interactions between different buckling modes. The primary objective is to develop design procedures that improve structural engineering practices. Thin-walled CFS columns are susceptible to local, distortional, and global buckling (L, D, and G), as well as their interactions (LG, LD, DG and LDG). These interactions occur in many forms, driven by the distinct structural behavior of each mode, which is characterized by different buckling shapes and post-critical responses. Numerical studies conducted by the authors have resulted in an original "all-in-one" design procedure for CFS lipped channel columns affected by LG, LD, DG or LDG buckling interactions. This procedure builds upon the current Direct Strength Method (DSM) and integrates the authors' previous solutions for LD interaction. The reliability of the proposed approach in comparison with experimental results from the literature was analyzed using the First-Order Second-Moment (FOSM) method, the First-Order Reliability Method (FORM) and the Monte Carlo simulation. In all instances, the reliability index obtained exceeded the target index ( $\beta_0$ ), justifying an increase in the resistance factor ( $\phi$ ). The reliability analysis also demonstrated that the proposed design procedures outperform the existing design equations in current codes.

### **1. Introduction**

Cold-formed steel (CFS) members offer significant versatility due to their outstanding strength-to-weight ratio. This benefit is achieved by adding folds to thin steel sheets, which enhances their structural performance for common engineering applications. Figure 1 shows the most commonly used cross-sections, including: (a) Lipped channel, (b) Hat, (c) Zed and (d) Rack. These sections are extensively used in light steel framing construction systems, where they may be subjected to compression and bending, as columns, beams and trussed systems.

---

<sup>1</sup> Professor, Federal University of Rio de Janeiro, batista@coc.ufrj.br

<sup>2</sup> Postdoctoral researcher, State University of Maringá, gustavoyoshio@coc.ufrj.br

<sup>3</sup> Professor, Federal University of Ouro Preto, marcilio@ufop.edu.br

<sup>4</sup> DSc student, Federal University of Ouro Preto, victor.amf@aluno.ufop.edu.br

<sup>5</sup> Associate Professor, Federal University of Itajubá, andrerieira@unifei.edu.br

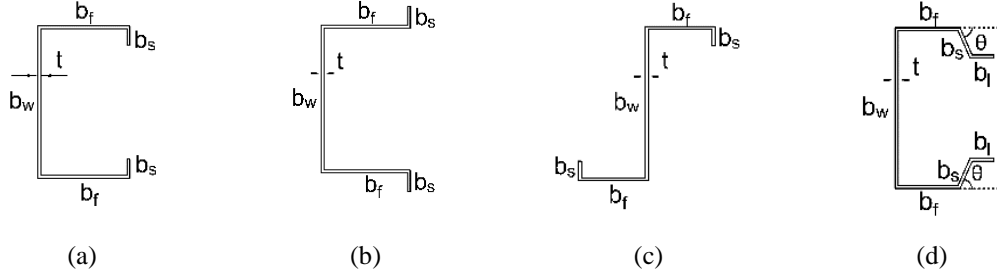


Figure 1. Cold-formed steel sections (CFS): (a) Lipped channel, (b) Hat, (c) Zed, (d) Rack

The Direct Strength Method (DSM) proposed by Schafer and Peköz (Schafer and Peköz 1998) is one of the primary structural design methods, implemented in standards such as the American Iron and Steel Institute (AISI 2016), the Australian/New Zealand Standard (AS/NZS 2018) and the Brazilian Association of Technical Codes (ABNT 2010). This method provides a straightforward and practical design approach, supported by the computational software to determine the critical buckling loads. Examples of such software include GBTUL (Bebiano, Gonçalves and Camotim 2015), CUFSM (Li and Schafer 2010), THIN-WALL-2 (Papangelis and Hancock 1995) and FStr (Lazzari and Batista 2021).

The DSM outlines procedures for designing columns and beams under local (L), distortional (D) and global (G) buckling modes, including the interaction between local and global buckling (LG). However, there remains a need to develop design procedures that address other buckling interactions: (i) local-distortional (LD), (ii) distortional-global (DG) and (iii) the triple local-distortional-global (LDG) buckling modes interaction. The present study developed DSM-based design methodologies by including the additional buckling modes effects from LD and LDG interactions. For this, the authors firstly studied the importance of these buckling modes interactions, in order to define whether they are actually important to be taken into consideration.

Both experimental and finite element method results were considered to test different approaches for the design of CFS thin-walled columns. After realizing that the current DSM equations are not able to capture the effects of the LD and LDG interactions, original sets of equations were proposed and compared with the experimental and numerical data bases. It was decided that the proposed design solutions must fulfill the following principles: (i) based on the DSM conception, which means refined comprehension of the buckling behavior of the member, allowing the access to the CFS section signature curve with the help of computational results of the critical buckling loads and shapes, which can be activated with the above cited softwares GBTUL, CUFSM, THIN-WALL-2 or FStr; (ii) keep the usual way to handle the buckling behavior of the member with the parametric slenderness ratio factors related to each buckling mode L, D and G, as well as the buckling interactions LG, LD and LDG, respectively  $\lambda_L$ ,  $\lambda_D$ ,  $\lambda_G$ ,  $\lambda_{LG}$ ,  $\lambda_{LD}$  and  $\lambda_{LDG}$ ; (iii) the set of equations must be easily understood and applied by means of handmade or data sheet calculation.

## 2. Direct Strength Method (DSM)

The Direct Strength Method (DSM) (Schafer and Peköz 1998) offers a straightforward approach for designing CFS columns subjected to single local, distortional and global buckling, as well as the local-global buckling mode interaction LG.

Equation 1.a of the DSM describes a Winter-type curve used for the structural design of columns under LG buckling interaction, and Eqs. 1.b and 1.c are related to the global buckling of the column. The local and global buckling loads are  $P_L$  and  $P_G$ , respectively, while the squash load is represented by  $P_y = A_s P_y$ , with  $A_s$  as the cross-sectional area and  $f_y$  as the steel yield stress.

$$P_{nLG} = \begin{cases} P_{nG} & \lambda_{LG} \leq 0.776 \\ \left(1 - \frac{0.15}{\lambda_{LG}^{0.8}}\right) \frac{P_{nG}}{\lambda_{LG}^{0.8}} & \lambda_{LG} > 0.776 \end{cases} \quad \text{with} \quad \lambda_{LG} = \sqrt{\frac{P_{nG}}{P_L}} \quad (1.a)$$

$$\chi_n = \begin{cases} (0.658(\lambda_G)^2) & \lambda_G \leq 1.50 \\ \left(\frac{0.877}{\lambda_G^2}\right) & \lambda_G > 1.50 \end{cases} \quad \text{with} \quad \lambda_G = \sqrt{\frac{P_y}{P_G}} \quad (1.b)$$

$$P_{nG} = \chi_n P_y \quad (1.c)$$

Additionally, Eq. 2 describes a Winter-type curve used for designing columns under the distortional buckling mode. The DSM design strength is defined as the lower value between Eqs. 1 and 2,  $P_{nDSM} = \min \{P_{nLG}, P_{nD}\}$ .

$$P_{nD} = \begin{cases} P_y & \lambda_D \leq 0.561 \\ \left(1 - \frac{0.25}{\lambda_D^{1.2}}\right) \frac{P_y}{\lambda_D^{1.2}} & \lambda_D > 0.561 \end{cases} \quad \text{with} \quad \lambda_D = \sqrt{\frac{P_y}{P_D}} \quad (2)$$

### 3. Modified DSM with the inclusion of the Local-Distortional buckling modes interaction

The first step of the present study was the identification and verification of the actual importance of the local-distortional buckling interaction behavior, LD, for CFS thin-walled columns, and the solution for practical design (Matsubara and Batista 2023). Figure 2 shows the comparison between experimental results,  $P_{exp}$ , and the current DSM design approach  $P_{nDSM}$  (Eqs. 1 and 2) of a series of lipped channel (LC) columns. These results are illustrated as  $P_{exp}/P_{nDSM}$  vs.  $R_{\lambda DL}$ , with the variable  $R_{\lambda DL} = \lambda_D/\lambda_L$  as the ratio between D and L slenderness ratio factors and the reported failure modes are identified. It is clear that the DSM strength results remain on the unsafe side for a large number of test results.

Additional FEM results are shown in Fig. 3, with  $P_{FEM}/P_{nDSM}$  vs.  $R_{\lambda DL}$ , for the case of LC columns affected by the LD buckling interaction. It is possible to observe the same tendency as indicated by previous experimental results, with clear region displaying unsafe results from the DSM equations. Based on these results, the authors defined a region mostly affected by the LD interaction, for the  $R_{\lambda DL}$  variable interval:  $0.45 \leq R_{\lambda DL} \leq 1.05$ . This definition is, of course, an approximated definition that was confirmed later as an acceptable choice, by the results of the comparisons of the proposed LD design approach with both experimental and FEM results.

Finally, the variable  $R_{\lambda DL}$  was defined as the main variable of the problem of the LD buckling interaction. This definition proved to be a reasonable choice, in accordance with the usual design practice, based on the slenderness ratio factors.

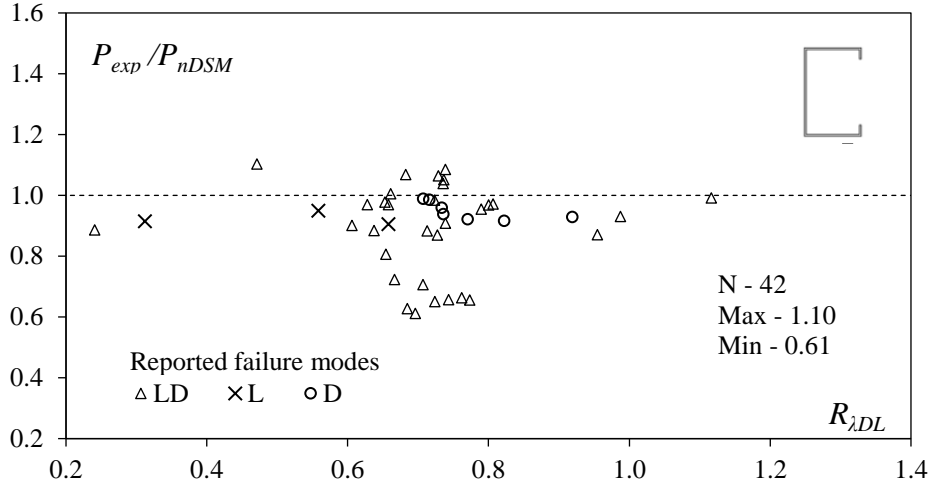


Figure 2. Comparison between experimental and the current DSM approach results, for lipped channel columns affected by the LD buckling interaction, with experimental results from (Kwon and Hancock 1992), (Loughlan, *et al.* 2012), (Chen *et al.* 2019), (Huang *et al.* 2021), (Lau and Hancock 1988), (Young and Rasmussen 1998), (Young *et al.* 2013)

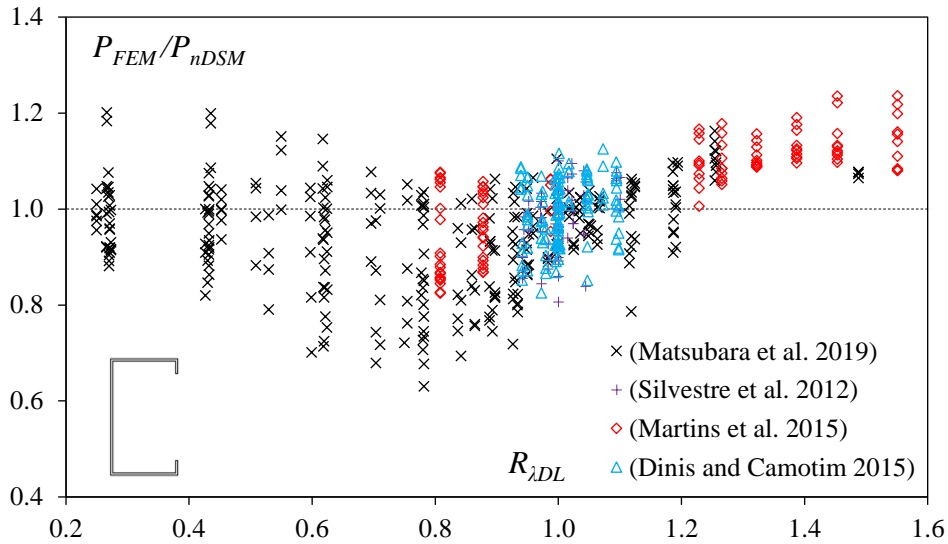


Figure 3. Comparison between FEM and the current DSM approach results, for lipped channel columns affected by the LD buckling interaction, with FEM results from (Matsubara *et al.* 2019), (Silvestre *et al.* 2012), (Martins *et al.* 2015), (Dinis and Camotim 2015)

The proposed set of equations to solve the LD structural design of CFS columns,  $P_{nLD}$ , is presented by Eqs. 3 to 6, which configures the strength surface presented in Fig. 4. One may confirm that the proposed equations include the LD solution in between the current DSM solutions for L and D single buckling strength, with (i)  $P_{nLD} = P_{nL}$  for  $R_{\lambda DL} < 0.45$ , (ii)  $P_{nLD} = P_{nD}$  for  $R_{\lambda DL} > 1.05$ , with  $P_{nL}$  from Eq. 1.a by replacing  $P_{nG}$  by  $P_y$ , and  $P_{nD}$  from Eq. 2. For these two cases of single L and D buckling with no interaction behavior, the variables  $a$  and  $b$  in Eq. 5 and 6 converge to 0.15 and 0.8 for the case of local buckling, and 0.25 and 1.2 for distortional buckling column strengths.

Finally, the proposed LD buckling interaction strength surface is valid for the case of columns with limited global buckling slenderness ratio factor,  $\lambda_G$ , in order to avoid the effect of the interaction between the three buckling modes, L, D and G. For this, the proposed approach was

tested with experimental and FEM results of columns with limited slenderness factor ratio  $\lambda_G/\lambda_{maxLD} \leq 0.4$ .

$$P_{nLD} = \begin{cases} P_y = A_s f_y & \text{for } \lambda_{maxLD} \leq \lambda_{limLD} \\ \left(1 - \frac{a}{\lambda_{maxLD}^b}\right) \frac{P_y}{\lambda_{maxLD}^b} & \text{for } \lambda_{maxLD} > \lambda_{limLD} \end{cases} \quad (3)$$

$$\text{with } \lambda_{maxLD} = \max(\lambda_L, \lambda_D) \quad (4.a)$$

$$\lambda_{limLD} = \sqrt[b]{0.5 + \sqrt{0.25 - a}} \quad (4.b)$$

$$\text{and } R_{\lambda DL} = \lambda_D / \lambda_L \quad (4.c)$$

$$a = \begin{cases} 0.15 & R_{\lambda DL} < 0.80 \\ 0.40 R_{\lambda DL} - 0.17 & 0.80 \leq R_{\lambda DL} \leq 1.05 \\ 0.25 & R_{\lambda DL} > 1.05 \end{cases} \quad (5)$$

$$b = \begin{cases} 0.80 & R_{\lambda DL} < 0.45 \\ -2.26 R_{\lambda DL}^2 + 4.06 R_{\lambda DL} - 0.57 & 0.45 \leq R_{\lambda DL} \leq 1.05 \\ 1.20 & R_{\lambda DL} > 1.05 \end{cases} \quad (6)$$

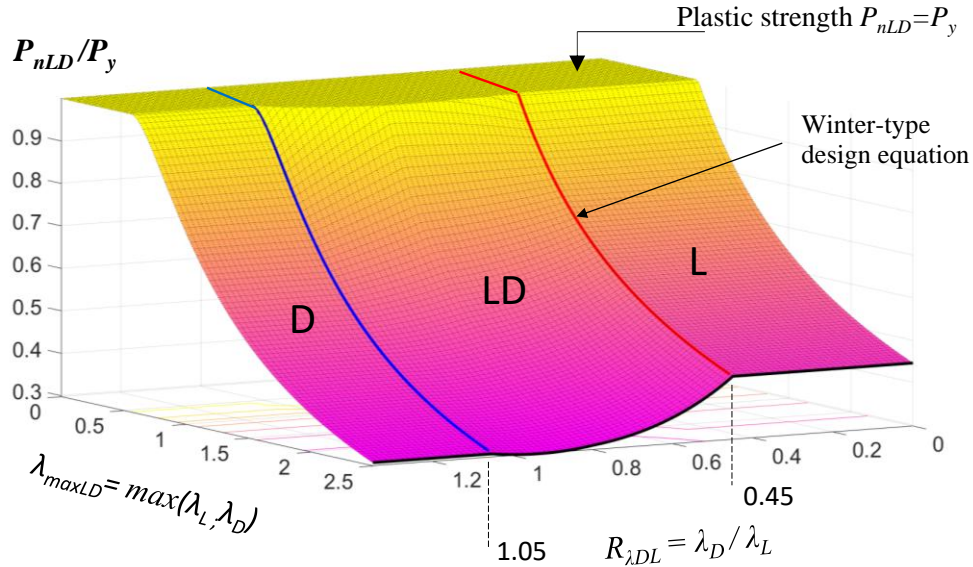


Figure 4. CFS thin-walled column strength surface for the case of LD buckling interaction. Valid for the case of the global buckling fully excluded (Matsubara and Batista 2023)

The proposed solution for LD buckling interaction of Eqs. 3 to 6 was tested for Lipped channel, Hat, Zed and Rack plain sections (Racks with no perforations) and the results were satisfactory, proving the design solution can be easily applied, displays safe results and improves the current DSM approach. The reliability analysis was conducted based on the LRFD method expressed by Eq. 7, with the dead to live loads ratio  $D/L = 0.20$ , and the loads combination  $1.2D + 1.6L$ . In addition, the usual parameters included in the current AISI standard (AISI 2020) were considered

in the analysis, with (i)  $C_\phi=1.52$  as the LRFD correction factor, (ii)  $M_m=1.10$  is the mean material factor, (iii)  $F_m=1.00$  is the mean fabrication factor, (iv)  $V_M=0.10$  is the coefficient of variation of the material factor, (v)  $V_F=0.05$  is the coefficient of variation of the fabrication factor, (vi)  $C_p$  is the correction factor related to the number of test results, (vii)  $\beta_0=2.50$  is the target reliability index for the case of structural members, (viii)  $V_Q=0.21$  is the load effect coefficient of variation, and (ix)  $P_m$  and  $V_p$  are the mean and the coefficient of variation of the exact-to-predicted failure load ratios.

$$\phi = C_\phi M_m F_m P_m e^{-\beta_0 \sqrt{V_M^2 + V_F^2 + C_p V_p^2 + V_Q^2}} \quad (7)$$

Table 1 shows the reliability results for the FEM data set for LC, Hat, Zed and Rack plain CFS section columns, showing that it is possible to consider a higher safety factor, compared with the current DSM approach of Eqs. 1 and 2. This improvement can be accomplished by replacing the single distortional buckling Eq. 2 with the proposed LD buckling interaction solution of Eqs.3 to 6.

In addition, Fig. 5 shows the results of the comparison between FEM and the proposed design approach,  $P_{FEM}/P_{nLD}$ , for the case of lipped channel (LC) CFS columns. The comparison of the results of Fig. 5 ( $P_{FEM}/P_{nLD}$  vs.  $R_{\lambda DL}$ ) with those in Fig. 3, ( $P_{FEM}/P_{nDSM}$  vs.  $R_{\lambda DL}$ ) shows the clear improvement promoted by the proposed LD design solution.

Table 1. Reliability results of the proposed design approach for LD buckling interaction, Eqs. 3 to 6, for FEM data

Section-type	N	Mean	St. Dev.	Coef. Var.	Safety factor $\phi$
LC	593	1.02	0.08	0.08	0.91
Hat	426	1.06	0.06	0.06	0.96
Zed	446	1.06	0.06	0.06	0.96
Rack	470	1.04	0.10	0.10	0.92

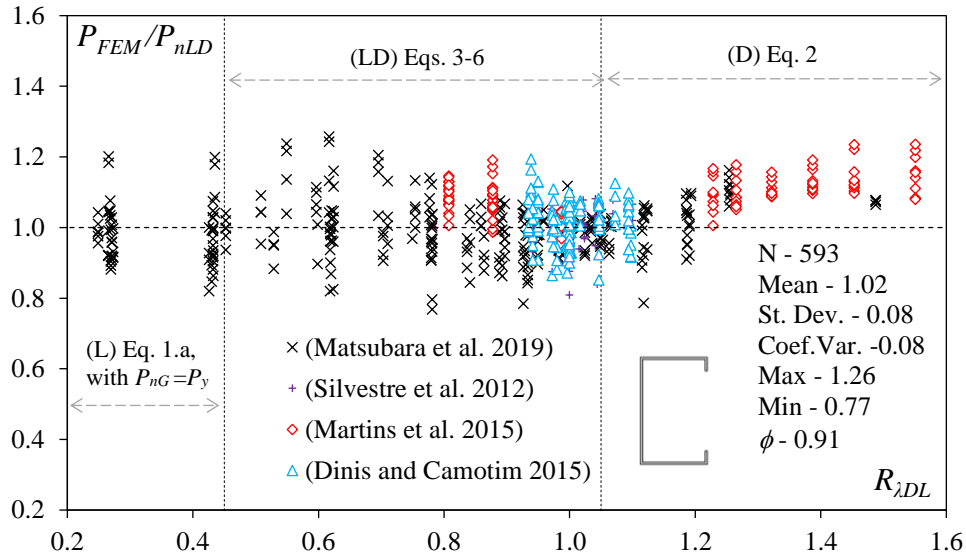


Figure 5. Results of the comparison between FEM and the proposed design results,  $P_{u,FEM}/P_{nLD}$ , of lipped channel (LC) CFS columns, related to the main variable of the problem  $R_{\lambda DL} = \lambda_D/\lambda_L$  (Matsubara and Batista 2023)

#### 4. “All-in-one” design approach - Generalized Direct Strength Method

The Generalized Direct Strength Method (GDSM), initially developed by Matsubara, Batista and Salles (Matsubara *et al.* 2019), was only addressed to the combinations of the LG and LD buckling interaction solutions, the former from the current DSM (Eqs. 1 and 2) and the latter as presented above (Eqs. 3 to 6). The GDSM incorporating LG and LD buckling interactions has been further refined in more recent reported research (Matsubara and Batista 2023). This CFS column design method is based on a finite element parametric study conducted using the FEM software package ANSYS (SAS IP INC. 2009). The thin-shell finite element model was described in previous works of the research group, (Matsubara *et al.* 2019) and (Matsubara and Batista 2023), and the analysis of CFS thin-walled columns were performed based on the concept of the GMNIA strategy (Geometrically and Materially Nonlinear Analysis with Imperfections).

More recently, the GDSM has incorporated the global mode into its methodology (Matsubara and Batista 2022), expanding its scope to include DG and LDG interactions, thereby providing a comprehensive "all-in-one" approach described by Eqs. 8 to 17, with the variables  $a$  and  $b$  defined by Eqs. 5 and 6, and  $\chi_n$  by Eq. 1.b. This advancement led to the development of the strength surface  $P_{nLDG}$  vs.  $(R_{\lambda DL}, \lambda_{LDG}, \lambda_G)$ , with the main variable  $R_{\lambda DL} = \lambda_D/\lambda_L$ , along with the variables  $\lambda_{LDG}$  (Eq. 9),  $\lambda_{maxLD}$  (Eq. 10),  $\lambda_{limLDG}$  (Eq. 11) and  $\lambda_G$ .

$$P_{nLDG} = \begin{cases} P_{nG} = \chi_n P_y & \text{for } \lambda_{LDG} \leq \lambda_{limLDG} \\ \left(1 - \frac{a}{\lambda_{LDG}^b}\right) \frac{\chi_m P_y}{\lambda_{LDG}^b} & \text{for } \lambda_{LDG} > \lambda_{limLDG} \end{cases} \quad (8)$$

$$\text{with } \lambda_{LDG} = \lambda_{maxLD} \sqrt{\chi_m} \quad (9)$$

$$\lambda_{maxLD} = \max(\lambda_L; \lambda_D) \quad (10)$$

$$\text{and } \lambda_{limLDG} = \sqrt[b]{0.5\mu + \sqrt{0.25\mu^2 - a\mu}} \quad (11)$$

$$\chi_m = \begin{cases} \left(c(\lambda_G)^d\right) & \lambda_G \leq 1.50 \\ \left(\frac{e}{(\lambda_G)^f}\right) & \lambda_G > 1.50 \end{cases} \quad (12)$$

$$\mu = \frac{\chi_m}{\chi_n} \geq 1.0 \quad (13)$$

$$c = \begin{cases} 0.66 & R_{\lambda DL} < 0.45 \\ 0.20R_{\lambda DL} + 0.57 & 0.45 \leq R_{\lambda DL} \leq 1.65 \\ 0.90 & R_{\lambda DL} > 1.65 \end{cases} \quad (14)$$

$$d = \begin{cases} 2.00 & R_{\lambda DL} < 0.45 \\ 0.20R_{\lambda DL} + 1.91 & 0.45 \leq R_{\lambda DL} \leq 1.65 \\ 2.24 & R_{\lambda DL} > 1.65 \end{cases} \quad (15)$$

$$e = \begin{cases} 0.88 & R_{\lambda DL} < 0.45 \\ 0.35R_{\lambda DL} + 0.72 & 0.45 \leq R_{\lambda DL} \leq 1.65 \\ 1.30 & R_{\lambda DL} > 1.65 \end{cases} \quad (16)$$

$$f = \begin{cases} 2.00 & R_{\lambda DL} < 0.55 \\ -0.59R_{\lambda DL} + 2.32 & 0.55 \leq R_{\lambda DL} \leq 1.65 \\ 1.35 & R_{\lambda DL} > 1.65 \end{cases} \quad (17)$$

A key point to highlight the  $P_{nLDG}$  column strength conception is that Eqs. 8 and 12 preserve the fundamental equations' arrangement of the DSM, as described by Eq. 1. It can be observed that for  $R_{\lambda DL} < 0.45$ , Eq. 8 aligns with Equation 1, resulting in  $P_{nLDG} = P_{nLG}$ . Additionally, for columns where  $R_{\lambda DL} > 1.05$  and the values of  $\lambda_G$  are low, indicating minimal influence of the global mode ( $\chi_m \cong \chi_n \cong 1$ ), the Eq. 8 aligns with Eq. 2, with  $P_{nLDG} = P_{nD}$ .

The GDSM methodology (Eqs. 8 to 17) was initially calibrated for CFS thin-walled lipped channel columns. Additional FEM tests were performed with a series of Zed columns, showing the proposed method is able to be applied for the design of this type of column.

Figure 6 illustrates the CFS column strength surface of Eqs. 8 to 17 for the specific case of  $R_{\lambda DL} = 1.0$ . It is important to note that this methodology generates multiple Winter-type curves in the plane  $P_{nLDG}$  vs.  $\lambda_{LDG}$ , according to the original formulation established by the Direct Strength Method.

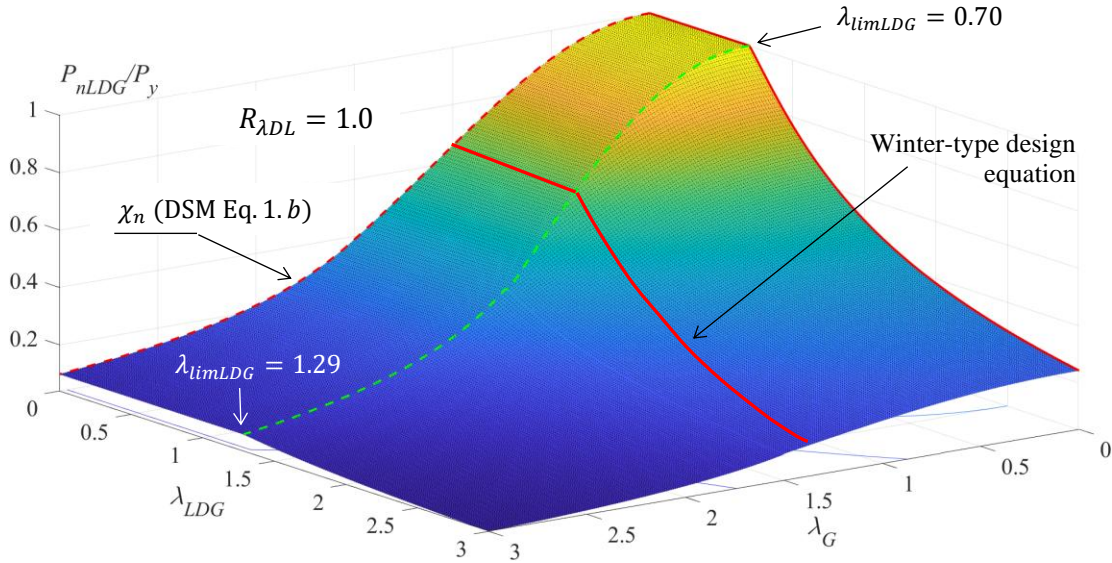


Figure 6: Example of the proposed column strength surface  $P_{nLDG}$  defined by Eqs. 8 to 17, for the particular case of  $R_{\lambda DL} = \lambda_D/\lambda_L = 1.0$

The methodology of the Generalized Direct Strength Approach,  $P_{nLDG}$ , is thoroughly detailed in the flowchart shown in Fig. 7.



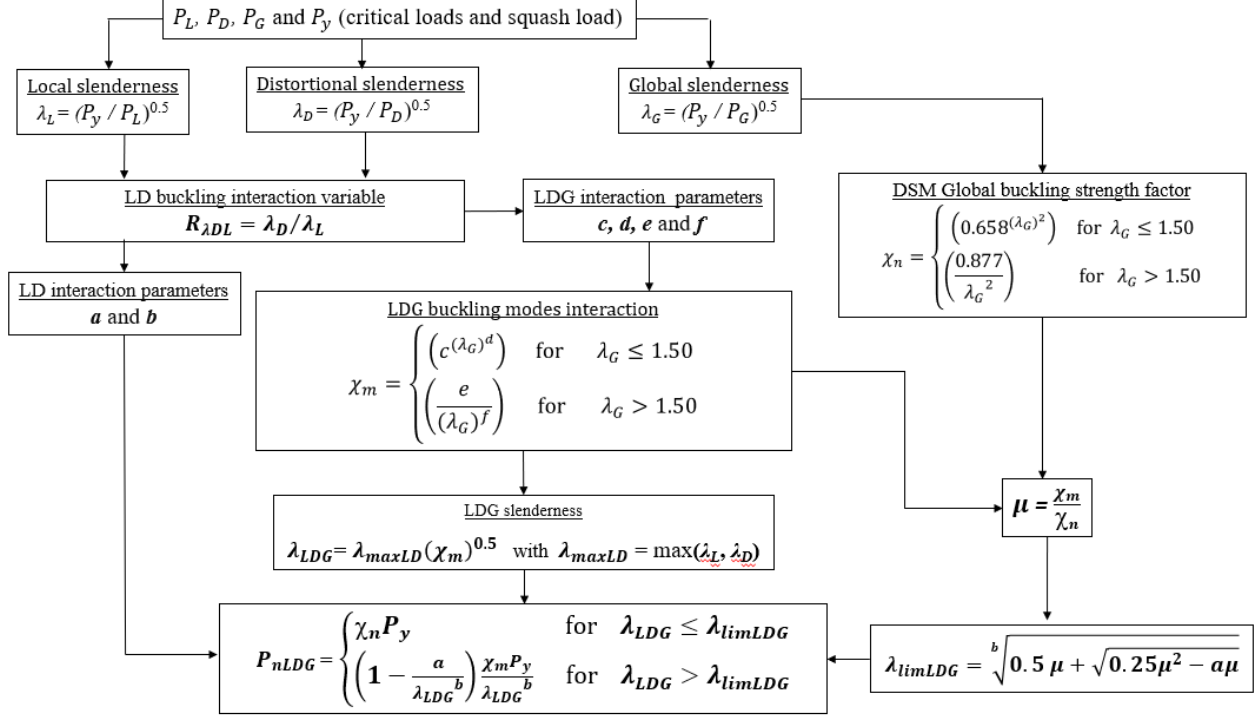


Figure 7: GDSM flowchart for the computation of CFS lipped channel column strength  $P_{nLDG}$

Two practical design examples of LC columns are included in the Appendix, according with the current DSM, the LD buckling interaction and the general LDG approaches, respectively  $P_{nDSM}$ ,  $P_{nLD}$  and  $P_{nLDG}$ . These examples explore the results of a thin-walled LC 200x75x20x1.5mm section ( $\lambda_L = 2.22$  and  $\lambda_D = 1.73$ ), with column lengths  $L$  of 1000 and 2500mm, with  $\lambda_G = 0.62$  and 1.91, respectively. The material properties are  $E=210\text{GPa}$ ,  $\nu=0.3$  and  $f_y = 450\text{MPa}$ , Young modulus, Poisson's ratio and yielding stress, respectively. The presented examples show that both proposals to improve the design of CFS columns,  $P_{nLD}$  and  $P_{nLDG}$ , are easily applied, and are in close agreement with the original DSM methodological basis.

## 5. Experimental Assessment of the “All-in-one” design approach, GDSM

The assessment of the current DSM was performed with experimental LC column results, as presented in Fig. 8, with the test data characterized according to the reported failure modes, as reported by (Young *et al.* 2013), (Young and Rasmussen 1998), (Salles 2017), (Kwon and Hancock 1992) (Loughlan *et al.* 2012), (Lau and Hancock 1988), (Chen *et al.* 2019), (Young *et al.* 2018), (Santos 2014), (Huang *et al.* 2021), (Heva and Mahendran 2013) and (Jayasidhan *et al.* 2023). Table 2 summarize the assembled database of experimental column tests.

It can be observed in Fig. 8 that the DSM produces a large distribution of the column strength ratio  $P_{exp}/P_{nDSM}$ , especially for the cases of LD, FT and LD+FT failures, respectively local-distortional, global flexural torsional and local-distortional-global FT. The statistical analysis shows a mean value of 1.00, coefficient of variation of 0.15.

Table 2: Experimental database description

Reference	Number of test results	$R_{\lambda DL}$	
		min	max
Young <i>et al.</i> (2013)	26	0.61	0.96
Young and Rasmussen (1998)	6	0.47	0.84
Salles (2017)	2	1.04	1.10
Kwon and Hancock (1992)	5	0.77	1.31
Loughlan <i>et al.</i> (2012)	5	0.63	0.75
Lau and Hancock (1988)	17	0.46	1.17
Chen <i>et al.</i> (2019)	3	0.16	0.31
Young <i>et al.</i> (2018)	17	0.86	1.06
Santos (2014)	32	0.92	1.22
Huang <i>et al.</i> (2021)	23	0.65	1.16
Heva and Mahendran (2013)	6	0.92	1.07
Jayasidhan <i>et al.</i> (2023)	3	1.40	1.46
Total	145		

Figure 9 presents the comparison between the same experimental data results of Fig. 8, with the GDSM proposed approach of Eqs. 8 to 17,  $P_{exp}/P_{nLDG}$ . It can be observed that the GDSM clearly improves the strength results when compared with those from the DSM in Fig. 8, resulting in statistical results with a mean of 1.02 and coefficient of variation of 0.11. These results show (i) important improvement of columns with LD failure, (ii) moderate improvement of LDG (L+D+FT) failures and (ii) null change for the case of columns with failure in single flexural torsional (FT) buckling. The latter condition was explained by (Dinis *et al.* 2020), which concluded that Eqs. 1.b and 1.c conduct to conservative design for LC columns developing FT buckling for the case of  $\lambda_G > 1.50$ . However, the authors of the present investigation consider that such cases of quite slender columns are relatively uncommon and that modifying the proposed strength equations would be unnecessary.

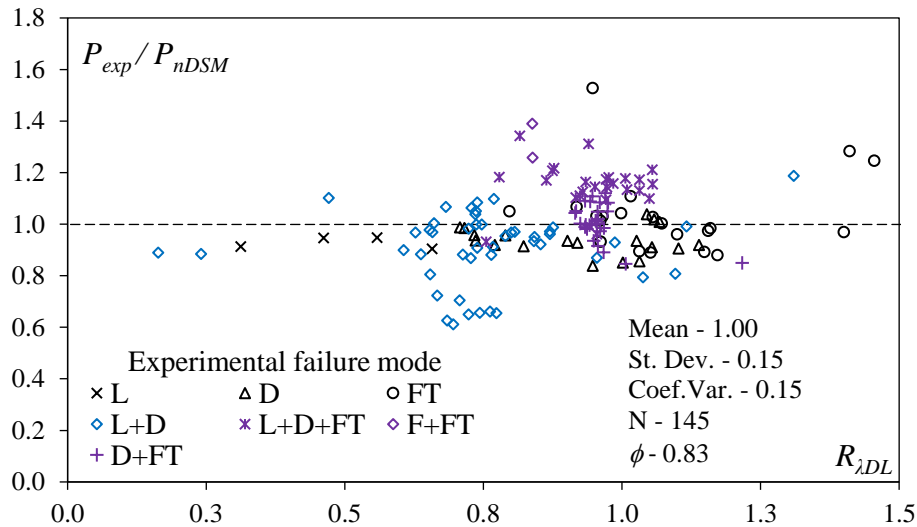


Figure 8: Comparison between experimental results and the current DSM equations (Eqs. 1 and 2), related to the slenderness factors ratio variable  $R_{\lambda DL} = \lambda_D/\lambda_L$

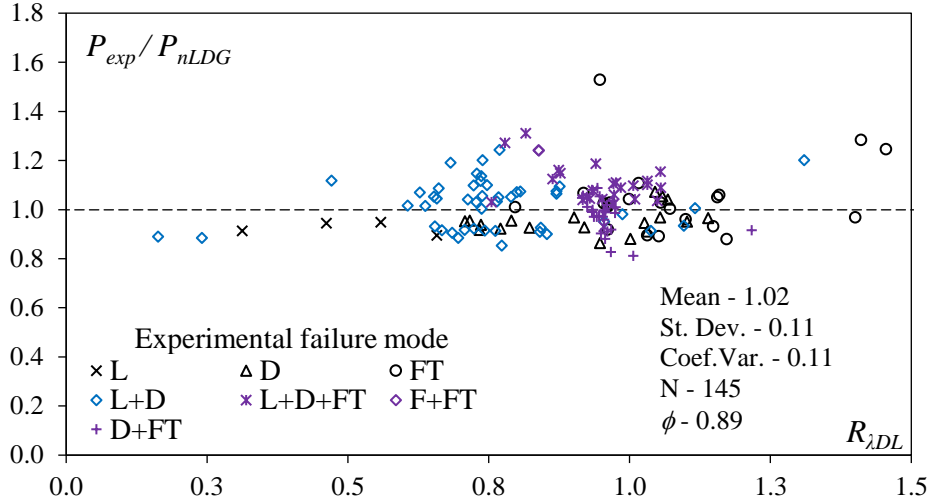


Figure 9: Comparison between experimental results and the proposed GDSM approach (Eqs. 8 to 17), related to the slenderness factors ratio variable  $R_{\lambda DL} = \lambda_D / \lambda_L$

## 6. Structural reliability analysis

To be applied in the CFS column design process, the GDSM needs to have a proper resistance factor for the structural design codes based on the limit states criteria. Together with the load factors, the resistance factor needs to meet safety requirements. In standards such as the LRFD-based AISI S100 (AISI 2020) and NBR 14762 (ABNT 2010), the safety parameter is the reliability index  $\beta$ , directly related to the probability of failure  $P_f$  by the cumulative standard normal density function  $\Phi$  in Eq. 18. Both standards establish a target reliability index of  $\beta_0 = 2.5$  for columns. For ultimate limit states, Eq. 19 shows the design condition to be satisfied, where  $\gamma_i$  are the load combination factors,  $\phi = 0.85$  and  $\gamma = 1.20$  are, respectively, the AISI S100 and NBR14762 resistance factors, for members in axial compression.

$$P_f = \Phi(-\beta_0) \quad (18)$$

$$\phi R = R / \gamma \geq \sum \gamma_i S_i \quad (19)$$

Considering only dead (D) and live (L) loads combination, the limit state function is shown in Eq. 20. The resistance is assumed to take the form of  $R = R_n(PMF)$ , where  $P$ ,  $M$  and  $F$  factors represent the ratio between actual and nominal values of the resistance (Professional factor  $P$ ), material properties ( $M$ ) and cross sectional properties (Fabrication factor  $F$ ) (Ellingwood *et al.* 1980). The random variables parameters are described in Table 3. For the professional factor statistics, the column strength from the experimental database in Table 2 was adopted. The resistance values were compared to the nominal strengths  $P_{nDSM}$  (DSM) and  $P_{nLDG}$  (GDSM).

$$R_n(P, M, F) \geq D + L \quad (20)$$

Table 3: Statistics for the reliability analysis

Variable	Mean	Coefficient of variation	Distribution	Reference
$P_{exp}/P_{nDSM}$ (DSM)	1.00	0.15	Normal	-
$P_{exp}/P_{nLDG}$ (GDSM)	1.02	0.11	Lognormal	-
$M$	1.10	0.10	Lognormal	(Ravindra and Galambos 1978)
$F$	1.00	0.05	Lognormal	(Ravindra and Galambos 1978)
$D$	$1.05D_n$	0.10	Normal	(Galambos <i>et al.</i> 1982)
$L$	$1.00L_n$	0.25	Extreme Type I	(Galambos <i>et al.</i> 1982)

For the nominal resistance in Eq. 19, the columns were considered designed just at its ultimate limit state, so that  $\phi R_n = R_n/\gamma = \gamma_D D_n + \gamma_L L_n$ . The AISI S100 (AISI 2016) LRFD load combination for this case is  $1.2D_n + 1.6L_n$ , and for the Brazilian code NBR 14762 (ABNT 2010), the  $1.35D_n + 1.5L_n$  combination is to be adopted in a 2025 revised version, therefore it was used herein. The live-to-dead load ratio adopted for both load combinations is  $L_n/D_n = 5$ , based on previous calibrations (Hsiao *et al.* 1990; Ganesan and Moen 2012).

### 6.1 Reliability analysis using the First-Order Second-Moment (FOSM) method

The first method used to derive the reliability indices is the First-Order Second-Moment (FOSM). Both resistance  $R$  and load effect  $S$  are assumed to follow the lognormal probability distribution, so that the reliability index can be obtained by Eq. 21 (Ellingwood *et al.* 1980).

$$\beta = \frac{\ln(R_m/S_m)}{\sqrt{V_R^2 + V_S^2}} \quad (21)$$

### 6.2 Reliability analysis using the First-Order Reliability Method (FORM)

The First-Order Reliability Method (FORM) represents the advanced FOSM method from (Hasofer and Lind 1974) adapted for non-normal random variables by (Rackwitz and Fiessler 1976). FORM obtains the reliability index in the space of the equivalent normal variables in an optimization process (Rackwitz and Fiessler 1978) to find the minimum distance from the origin to the limit state surface (failure surface). In the present investigation, the VBA algorithm (Low and Tang 2004) was used to find the  $\beta$  values via FORM, considering the fitted probability distributions for  $P_{exp}/P_{nDSM}$  and  $P_{exp}/P_{nLDG}$  in Table 4.

### 6.3 Reliability analysis results using Monte Carlo simulation

The Monte Carlo simulation (MCS) technique was also used to find the  $\beta$  values for columns designed with both the LRFD AISI S100-16 and the ultimate limit state NBR 14762. From the chosen number of 500,000 sets of random variables, synthetic samples of  $M$ ,  $F$ ,  $P$ ,  $D$  and  $L$  were generated, based on its probabilistic characteristics. For each set, the limit state function was evaluated, with the probability of failure  $P_f$  obtained from the ratio between the number of sets where the failure was detected (Eq. 19 not satisfied) and the total number of sets. The reliability indices were easily obtained from the inverse form of Eq. 18.

### 6.4 Reliability analysis results

Table 4 shows the obtained reliability indices for the AISI S100-16 and the Brazilian code NBR 1476, for the current resistance factors of  $\phi = 0.85$  and  $\gamma = 1.20$ , respectively. For the DSM, the target of  $\beta_0 = 2.5$  was met at the LRFD by FOSM method, which was used for the calibration of

$\phi = 0.85$  at the 1991 version of the AISI S100 (Hsiao *et al.* 1990; AISI 1991). However, FORM and the Monte Carlo simulation indicated that the current reliability index is slightly below the target value. For the Brazilian code, the obtained  $\beta$  values did not meet the target for any of the three reliability methods. The calculated values for GDSM, on the other hand, are higher than the target value, with a substantial margin for both design codes. These findings agree with the lowest coefficient of variation of  $P_{exp}/P_{nLDG}$ , when compared to  $P_{exp}/P_{nDSM}$ , 0.11 and 0.15, respectively in Table 3.

Table 4: Calculated reliability indices

Design method	Reliability method	Combination			
		AISI-LRFD		NBR	
		$\beta$	$P_f$	$\beta$	$P_f$
DSM	FOSM	2.45	0.72%	2.38	0.86%
	FORM	2.38	0.86%	2.33	1.00%
	MCS <sub>(500,000)</sub>	2.33	0.98%	2.27	1.17%
GDSM	FOSM	2.71	0.34%	2.63	0.42%
	FORM	2.62	0.44%	2.56	0.52%
	MCS <sub>(500,000)</sub>	2.61	0.45%	2.56	0.52%

Figure 10 shows the values of the reliability indices for different load ratios  $L_n/D_n$ . The indices decrease as the  $L_n/D_n$  increases, showing a tendency to stabilize at constant values. Since the live load has a higher coefficient of variation than the dead load, the reliability indices decrease as the influence of the live load in the total load increases (*i.e.*, at higher  $L_n/D_n$  values). For the case of  $L_n/D_n = 5$  the reliability indices for DSM calculated by the FOSM method are close to the LRFD target value. However, FORM and MCS indicated values significantly lower than  $\beta_0 = 2.5$ . For the case of LRFD-based design, the reliability values for GDSM are higher than the target value across the entire range of the analyzed  $L_n/D_n$  ratio, indicating that the safety factor  $\phi$  can be calibrated for a higher value, with favorable result in the design of more economic structures.

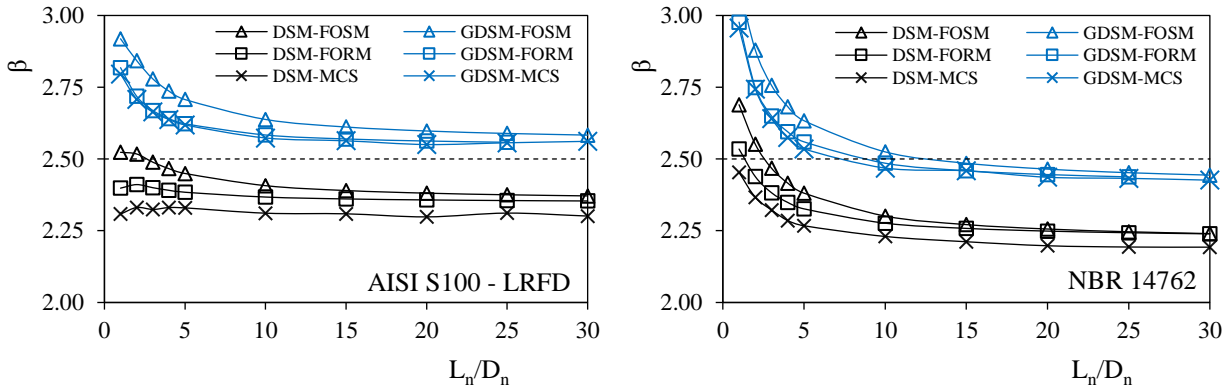


Figure 10: Results of the reliability index  $\beta$ , related to the loads ratio  $L_n/D_n$ , according to North American and Brazilian design codes for CFS lipped channel columns

### 6.5 Calibration of the resistance factor values

As presented in section 6.4, the current AISI LRFD resistance factor  $\phi = 0.85$  is suitable for the DSM when  $\beta$  was calculated by the FOSM method. For the GDSM the obtained reliability indices were considerably higher than the target value of  $\beta_0 = 2.5$ . To avoid an overly conservative design by GDSM, new resistance factors were calibrated for the target  $\beta_0 = 2.5$ . For that, an implemented

VBA algorithm (Microsoft Corporation 2016) was used to find  $\phi$  and  $\gamma$  values for the selected target. Table 5 shows the new calibrated resistance factors.

Table 5: Calibrated resistance factors

Design method	Reliability method	Combination	
		AISI-LRFD	NBR
DSM	FOSM	$\phi = 0.84$	$\gamma = 1.24$
	FORM	$\phi = 0.82$	$\gamma = 1.27$
GDSM	FOSM	$\phi = 0.90$	$\gamma = 1.16$
	FORM	$\phi = 0.88$	$\gamma = 1.18$

For both AISI S100 (AISI 2020) and NBR 14762 (ABNT 2010) design frameworks, the GDSM resistance factors are less conservative than the DSM one, which might provide more economic structures in the design process. The draft of the revised edition of the Brazilian code NBR 14762, to be published by 2025, includes both, the LD and the GDSM design methods of CFS columns: the former in the main text and the latter in an Appendix.

## 7. Final remarks

Firstly, it must be highlighted that the proposed GDSM,  $P_{nLDG}$ , is not only addressed to the design of columns displaying the triple buckling interaction LDG, but a general approach that includes all the failure modes, including the single buckling modes L, D and G, as well as the buckling interactions LG, LD and LDG. For this, the parameters  $a$  and  $b$  of Eqs. 5 and 6, and  $c$  to  $f$  of Eqs. 14 to 17, are able to converge to the current DSM equations for columns affected by single L, D or G buckling, as well as for the well established DSM LG buckling interaction solution (Eqs. 1 and 2). Depending on the parameters  $\lambda_{LDG} = \lambda_{maxLD}\sqrt{\chi_m}$  and  $\lambda_{limLDG}$ , which are related to the variables  $a$  to  $f$ , dependent of the main variable  $R_{\lambda DL}$ , the proposed strength surface of  $P_{nLDG}$  may conduct to both (i) the current DSM solutions for L, D and G and LG interaction, and (ii) the case of columns affected by the LD (mostly) or LDG (less frequent case) interaction.

It was found that the LD buckling interaction is the most important effect to be taken into consideration for design purposes, and the replacement of the D strength Eq. 2 by the proposed LD Eqs. 3 to 6 offers a significant improvement in the design results of CFS thin-walled columns. The LD solution was calibrated for LC, Hat, Zed and Rack plain sections.

Regarding the reliability results, it was found that the GDSM showed a lower coefficient of variation than DSM for the professional factor (Table 4). It was also confirmed that the safety factors of  $\phi = 0.85$  (LRFD) and  $\gamma = 1.20$  (Brazilian code) are suitable for the current DSM, based on the adopted experimental database of LC columns.

The reliability indices obtained for the GDSM ( $P_{nLDG}$ ) in Table 4, are higher than the target reliability factor, with  $\beta > \beta_0 (= 2.5)$ . Finally, the results of the calibration performed in section 6.5 and presented in Table 5, indicate that the values of  $\phi = 0.89$  and  $\gamma = 1.17$  could be adopted for the proposed GDSM design approach, the former in the LRFD scenario and the latter for the Brazilian code NBR 14762 design framework.

## Acknowledgments

The second author gratefully acknowledges the financial support provided by the National Council for Scientific and Technological Development (CNPq), Brazil, through the Doctoral scholarship 141287/2019-5.

The fourth author extends sincere thanks for the financial support received from Fundação de Amparo à Pesquisa do Estado de Minas Gerais (FAPEMIG).

## References

- ABNT (2010). “NBR 14762: Design of cold-formed steel structures.” Rio de Janeiro, Brazil: Associação Brasileira de Normas Técnicas (*In Portuguese*).
- AISI (1991). “LRFD Cold-Formed Steel Design Manual.” Washington, USA: American Iron and Steel Institute.
- AISI (2016). “AISI S100-16: North American Specification for the Design of Cold-Formed Steel Structural Members.” Washington, USA: American Iron and Steel Institute.
- AISI (2020). “AISI S100-16: North American Specification for the Design of Cold-Formed Steel Structural Members.” Washington, USA: American Iron and Steel Institute.
- Australian/New Zealand Standard (2018). “AS/NZS 4600:2018: Cold-formed steel structures.” Wellington: Australian/New Zealand Standard.
- Bebiano, R., Gonçalves, R., Camotim, D. (2015). “A Cross-Section Analysis Procedure to Rationalise and Automate the Performance of GBT-Based Structural Analyses.” *Thin-Walled Structures* 92 (July):29–47. <https://doi.org/10.1016/j.tws.2015.02.017>.
- Chen, J., Chen, M., Young, B. (2019). “Compression Tests of Cold-Formed Steel C- and Z-Sections with Different Stiffeners.” *Journal of Structural Engineering* 145 (5): 04019022. [https://doi.org/10.1061/\(ASCE\)ST.1943-541X.0002305](https://doi.org/10.1061/(ASCE)ST.1943-541X.0002305).
- Dinis, P.B., and D. Camotim. (2015). “Cold-Formed Steel Columns Undergoing Local–Distortional Coupling: Behaviour and Direct Strength Prediction against Interactive Failure.” *Computers & Structures* 147 (January):181–208. <https://doi.org/10.1016/j.compstruc.2014.09.012>.
- Dinis, P. B., Camotim, D., Landesmann, A., Martins, A. D. (2020). “Improving the Direct Strength Method Prediction of Column Flexural-Torsional Failure Loads.” *Thin-Walled Structures* 148 (March):106461. <https://doi.org/10.1016/j.tws.2019.106461>.
- Ellingwood, B., Galambos, T.V., MacGregor, J. G. and Cornell, C. A. (1980). “Development of a Probability Based Load Criterion for American National Standard A58. NBS Special Publication 577.” Washington, DC: U.S. Department of Commerce.
- Ellingwood, B., Galambos, T.V., MacGregor, J. G. and Cornell, C. A. (1982). “Probability Based Load Criteria: Assessment of Current Design Practice.” *Journal Of The Structural Division*, 1409–26.
- Ganesan, K., Moen, C. D. (2012). “LRFD Resistance Factor for Cold-Formed Steel Compression Members.” *Journal of Constructional Steel Research* 72:261–66.
- Hasofer, A. M., Lind, N. C. (1974). “Exact and Invariant First Order Reliability Format.” *Journal of Engineering Mechanics Division* 100:111–21.
- Heva, Y. B., Mahendran, M. (2013). “Flexural-Torsional Buckling Tests of Cold-Formed Steel Compression Members at Elevated Temperatures.” *Steel and Composite Structures* 14 (3): 205–27. <https://doi.org/10.12989/SCS.2013.14.3.205>.

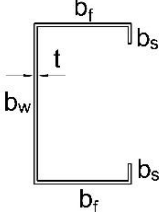
- Hsiao, L., Yu, W., Galambos, T.V. (1990). "AISI LRFD Method for Cold-Formed Steel Structural Members." *Journal of Structural Engineering* 116 (2): 500–517.
- Huang, L., Yang, W., Shi, T., Qu, J. (2021). "Local and Distortional Interaction Buckling of Cold-Formed Thin-Walled High Strength Lipped Channel Columns." *International Journal of Steel Structures* 21 (1): 244–59. <https://doi.org/10.1007/s13296-020-00436-z>.
- Jayasidhan, A.K., Kumar, M.V.A, Aswathy, K.C.K. (2023). "Experimental Investigation on Post-Flexural–Torsional Buckling Strength of CFS Compression Members." *Thin-Walled Structures* 185 (April):110638. <https://doi.org/10.1016/j.tws.2023.110638>.
- Kwon, Y. B., Hancock, G.J. (1992). "Tests of Cold-Formed Channels with Local and Distortional Buckling." *Journal of Structural Engineering* 118 (7): 1786–1803. [https://doi.org/10.1061/\(ASCE\)0733-9445\(1992\)118:7\(1786\)](https://doi.org/10.1061/(ASCE)0733-9445(1992)118:7(1786)).
- Lau, S.C.W., Hancock, G.J. (1988). "Distortional buckling tests of cold-formed channel sections." In *Specialty Conference on Cold-Formed Steel Structures*, 3:45–73. Missouri.
- Lazzari, J.A., Batista, E.M. (2021). "Finite Strip Method Computer Application for Buckling Analysis of Thin-Walled Structures with Arbitrary Cross-Sections." *REM - International Engineering Journal* 74 (3): 337–44. <https://doi.org/10.1590/0370-44672020740065>.
- Li, Z., Schafer, B.W. (2010). "Buckling Analysis of Cold-Formed Steel Members with General Boundary Conditions Using CUFSM: Conventional and Constrained Finite Strip Methods." In *Cold-Formed Steel Design and Construction*. Saint Louis, Missouri: Roger A. LaBoube e Wei-Wen Yu.
- Loughlan, J., Yidris, N., Jones, K. (2012). "The Failure of Thin-Walled Lipped Channel Compression Members Due to Coupled Local-Distortional Interactions and Material Yielding." *Thin-Walled Structures* 61 (December):14–21. <https://doi.org/10.1016/j.tws.2012.03.025>.
- Low, B.K., Tang, W.H. (2004). "Reliability Analysis Using Object-Oriented Constrained Optimization." *Structural Safety* 26 (1): 69–89.
- Martins, A.D., Dinis, P.B., Camotim, D., Providência, P. (2015). "On the Relevance of Local–Distortional Interaction Effects in the Behaviour and Design of Cold-Formed Steel Columns." *Computers & Structures* 160 (November):57–89. <https://doi.org/10.1016/j.compstruc.2015.08.003>.
- Matsubara, G. Y., Batista, E.M., Salles, G.C. (2019). "Lipped Channel Cold-Formed Steel Columns under Local-Distortional Buckling Mode Interaction." *Thin-Walled Structures* 137 (April):251–70. <https://doi.org/10.1016/j.tws.2018.12.041>.
- Matsubara, G.Y., Miranda Batista, E.M. (2023). "Local–Distortional Buckling Mode of Steel Cold-Formed Columns: Generalized Direct Strength Design Approach." *Thin-Walled Structures* 183 (February):110356. <https://doi.org/10.1016/j.tws.2022.110356>.
- Matsubara, G.Y., Batista, E.M. (2022). "CFS Columns Under Buckling Interaction: Direct Strength Method Generalised Approach." *Ce/Papers* 5 (4): 84–93. <https://doi.org/10.1002/cepa.1732>.
- Microsoft Corporation. (2016). "Microsoft Excel 2016."
- Papangelis, J.P., and G.J. Hancock. (1995). "Computer Analysis of Thin-Walled Structural Members." *Computers & Structures* 56 (1): 157–76. [https://doi.org/10.1016/0045-7949\(94\)00545-E](https://doi.org/10.1016/0045-7949(94)00545-E).
- Rackwitz, R., Fiessler, B. (1976). "Note on Discrete Safety Checking When Using Non-Normal Stochastic Models for Basic Variables. Load Project Working Session." Cambridge, Estados Unidos: Massachusetts Institute of Technology.
- Rackwitz, R., Fessler, B. (1978). "Structural Reliability under Combined Random Load Sequences." *Computers and Structures* 9 (5): 489–94.



- Ravindra, M. K., Galambos, T.V. (1978). "Load and Resistance Factor Design for Steel." *Journal of The Structural Division* 104 (9): 1337–53.
- Salles, G.C. (2017). "Analytical, numerical and experimental investigation of distortional buckling of cold-formed lipped channels". Master thesis, Civil Engineering Program, COPPE, Rio de Janeiro: Federal University of Rio de Janeiro (in Portuguese).
- Santos, E.S. (2014). "Local-distortional-global buckling interaction in cold-formed steel lipped channel columns". Ph.D. thesis, Civil Engineering Program, COPPE, Rio de Janeiro: Federal University of Rio de Janeiro (in Portuguese).
- SAS IP INC. (2009). "ANSYS." In *Theory Reference for the Mechanical APDL and Mechanical Applications*, 1:1190. Canonsburg, Pennsylvania: Peter Kohnke.
- Schafer, B.W., Peköz, T. (1998). "Direct Strength Prediction of Cold-Formed Steel Members Using Numerical Elastic Buckling Solutions." In , 1–8. St. Louis, Missouri: Department of Civil Engineering Center for Cold-formed Steel Structures University of Missouri.
- Silvestre, N., Camotim, D., Dinis, P.B. (2012). "Post-Buckling Behaviour and Direct Strength Design of Lipped Channel Columns Experiencing Local/Distortional Interaction." *Journal of Constructional Steel Research* 73 (June):12–30. <https://doi.org/10.1016/j.jcsr.2012.01.005>.
- Young, B., Dinis, P.B., Camotim, D. (2018). "CFS Lipped Channel Columns Affected by L-D-G Interaction. Part I: Experimental Investigation." *Computers & Structures* 207 (September):219–32. <https://doi.org/10.1016/j.compstruc.2017.03.016>.
- Young, B., Rasmussen, K.J.R. (1998). "Tests of Cold-Formed Channel Columns." In , 239–64. St. Louis, Missouri: Missouri University of Science and Technology.
- Young, B., Silvestre, N., Camotim, D. (2013). "Cold-Formed Steel Lipped Channel Columns Influenced by Local-Distortional Interaction: Strength and DSM Design." *Journal of Structural Engineering* 139 (6): 1059–74. [https://doi.org/10.1061/\(ASCE\)ST.1943-541X.0000694](https://doi.org/10.1061/(ASCE)ST.1943-541X.0000694).

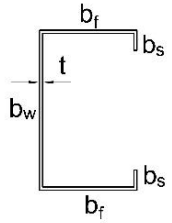
**APPENDIX:** Design examples of CFS lipped channel column

Example 1: Column not affected by the Global buckling, with  $\lambda_G/\max(\lambda_L, \lambda_D) = 0.22$ .  
LD buckling interaction leads the column behavior and strength.

<p>CFS LC 200 x 70 x 20 x 1.5 mm (<math>b_w \times b_f \times b_s \times t</math>)                  Out-out cross-section dimensions                  Geometric properties with sharp corners                  Cross-section area <math>A=561.0\text{mm}^2</math>                  Simply supported, pinned-pinned ends condition                  Column length <math>L=1000\text{mm}</math></p>	<p>Material:                  ASTM A572 Gr 65  <math>f_y=450\text{MPa}</math>  <math>E=210\text{GPa}</math>  <math>\nu = 0.3</math></p>	
---	---	---

LC 200 x 70 x 20 x 1.5 L=1000mm - Example 1					
Current DSM design		Proposal LD design		Proposal LDG design	
Critical buckling and plastic loads		Critical buckling and plastic loads		Critical buckling and plastic loads	
$P_L =$	32.6 kN	$P_L =$	32.6 kN	$P_L =$	32.62 kN
$P_D =$	79.1 kN	$P_D =$	79.1 kN	$P_D =$	79.07 kN
$P_G =$	653.5 kN	$P_G =$	653.5 kN	$P_G =$	653.5 kN
$P_y =$	252.5 kN	$P_y =$	252.5 kN	$P_y =$	252.5 kN
Slenderness factors		Slenderness factors		Slenderness factors	
$\lambda_L =$	2.78	$\lambda_L =$	2.78	$\lambda_L =$	2.78
$\lambda_D =$	1.79	$\lambda_D =$	1.79	$\lambda_D =$	1.79
$\lambda_G =$	0.62	$\lambda_G =$	0.62	$\lambda_G =$	0.62
Global buckling		Global buckling		Global buckling factor	
$\chi_n =$	0.85 (Eq. 1.b)	$\chi_n =$	0.85 (Eq. 1.b)	$\chi_n =$	0.85 (Eq. 1.b)
$P_{nG} = \chi_n P_y =$	214.8 kN	$P_{nG} = \chi_n P_y =$	214.8 kN	LDG buckling interaction	
LG buckling interaction		LG buckling interaction		$R_{\lambda DL} =$	0.64 (Eq. 4.c)
$\lambda_{LG} = (P_{nG} / P_L)^{0.5}$	2.57	$\lambda_{LG} =$	2.57	$a =$	0.15 (Eq. 5)
$P_{nLG} =$	93.9 kN (Eq. 1.a)	$P_{nLG} =$	93.9 kN (Eq. 1.a)	$b =$	1.11 (Eq. 6)
Distortional buckling		LD buckling interaction		$c =$	0.70 (Eq. 14)
$P_{nD} =$	110.1 kN (Eq. 2)	$R_{\lambda DL} =$	0.64 (Eq. 4.c)	$d =$	2.04 (Eq. 15)
Column strength		$a =$	0.15 (Eq. 5)	$e =$	0.94 (Eq. 16)
$P_{nDSM} = \min(P_{nLG}, P_{nD})$		$b =$	1.11 (Eq. 6)	$f =$	1.94 (Eq. 17)
$P_{nDSM} =$	<b>93.9</b> kN	$\lambda_{maxLD} =$	2.78 (Eq. 4.a)	$\chi_m =$	0.87 (Eq. 12)
		$\lambda_{limLD} =$	0.83 (Eq. 4.b)	$\mu =$	1.03 (Eq. 13)
Comparison of the design proposals		$P_{nLD} =$	77.5 kN (Eq. 3)	$\lambda_{limLDG} =$	0.86 (Eq. 11)
$P_{nDSM} / P_{nLD} =$	1.21	Column strength		$\lambda_{LDG} =$	2.60 (Eq. 9)
$P_{nDSM} / P_{nLDG} =$	1.29	$P_{nLD} = \min(P_{nLG}, P_{nLD})$		Column strength (Eq. 8)	
$P_{nLD} / P_{nLDG} =$	1.07	$P_{nLD} =$	<b>77.5</b> kN	$P_{nLDG} =$	<b>72.7</b> kN

**Example 2:** Column affected by the Global buckling, with  $\lambda_G/\max(\lambda_L, \lambda_D) = 0.76$ .  
 LG buckling interaction leads the column behavior and strength.

CFS LC 200 x 70 x 20 x 1.5 mm ( $b_w \times b_f \times b_s \times t$ ) Out-out cross-section dimensions Geometric properties with sharp corners Cross-section area $A=561.0\text{mm}^2$ Simply supported, pinned-pinned ends condition Column length $L=3500\text{mm}$	Material: ASTM A572 Gr 65 $f_y=450\text{MPa}$ $E=210\text{GPa}$ $\nu = 0.3$	
---	---	---

LC 200 x 70 x 20 x 1.5 L=3500mm - Example 2					
Current DSM design		Proposal LD design		Proposal LDG design	
Critical buckling and plastic loads		Critical buckling and plastic loads		Critical buckling and plastic loads	
$P_L =$	32.6 kN	$P_L =$	32.6 kN	$P_L =$	32.62 kN
$P_D =$	79.1 kN	$P_D =$	79.1 kN	$P_D =$	79.07 kN
$P_G =$	56.5 kN	$P_G =$	56.5 kN	$P_G =$	56.5 kN
$P_y =$	252.5 kN	$P_y =$	252.5 kN	$P_y =$	252.5 kN
Slenderness factors		Slenderness factors		Slenderness factors	
$\lambda_L =$	2.78	$\lambda_L =$	2.78	$\lambda_L =$	2.78
$\lambda_D =$	1.79	$\lambda_D =$	1.79	$\lambda_D =$	1.79
$\lambda_G =$	2.11	$\lambda_G =$	2.11	$\lambda_G =$	2.11
Global buckling		Global buckling		Global buckling factor	
$\chi_n =$	0.20 (Eq. 1.b)	$\chi_n =$	0.20 (Eq. 1.b)	$\chi_n =$	0.20 (Eq. 1.b)
$P_{nG} = \chi_n P_y =$	49.5 kN	$P_{nG} = \chi_n P_y =$	49.5 kN	LDG buckling interaction	
LG buckling interaction		LG buckling interaction		$R_{\lambda DL} =$	0.64 (Eq. 4.c)
$\lambda_{LG} = (P_{nG} / P_L)^{0.5}$	1.23	$\lambda_{LG} =$	1.23	$a =$	0.15 (Eq. 5)
$P_{nLG} =$	36.6 kN (Eq. 1.a)	$P_{nLG} =$	36.6 kN (Eq. 1.a)	$b =$	1.11 (Eq. 6)
Distortional buckling		LD buckling interaction		$c =$	0.70 (Eq. 14)
$P_{nD} =$	110.1 kN (Eq. 2)	$R_{\lambda DL} =$	0.64 (Eq. 4.c)	$d =$	2.04 (Eq. 15)
Column strength		$a =$	0.15 (Eq. 5)	$e =$	0.94 (Eq. 16)
$P_{nDSM} = \min(P_{nLG}, P_{nD})$		$b =$	1.11 (Eq. 6)	$f =$	1.94 (Eq. 17)
$P_{nDSM} =$	<b>36.6</b> kN	$\lambda_{maxLD} =$	2.78 (Eq. 4.a)	$\chi_m =$	0.22 (Eq. 12)
Comparison of the design proposals		$\lambda_{limLD} =$	0.83 (Eq. 4.b)	$\mu =$	1.13 (Eq. 13)
$P_{nDSM} / P_{nLD} =$	1.00	$P_{nLD} =$	77.5 kN (Eq. 3)	$\lambda_{limLDG} =$	0.95 (Eq. 11)
$P_{nDSM} / P_{nLDG} =$	0.99	Column strength		$\lambda_{LDG} =$	1.31 (Eq. 9)
$P_{nLD} / P_{nLDG} =$	0.99	$P_{nLD} = \min(P_{nLG}, P_{nLD})$		Column strength (Eq. 8)	
		$P_{nLD} =$	<b>36.6</b> kN	$P_{nLDG} =$	<b>36.8</b> kN